Energy 235 (2021) 121348

Contents lists available at ScienceDirect

Energy

journal homepage: www.elsevier.com/locate/energy

Hydrogen rich gas production through co-gasification of low rank coal, flotation concentrates and municipal refuse derived fuel

Adam Smoliński [a, *], Natalia Howaniec [b], Rafał Gąsior [c], Jarosław Polański [d], Małgorzata Magdziarczyk [e]

[a] Central Mining Institute, Plac Gwarkow 1, 40-166, Katowice, Poland
[b] Department of Energy Saving and Air Protection, Central Mining Institute, Plac Gwarkow 1, 40-166, Katowice, Poland
[c] Polish Mining Group, Powstancow 30, 40-039 Katowice, Poland
[d] Faculty of Science and Technology, Institute of Chemistry, University of Silesia, Szkolna 9, 40-006 Katowice, Poland
[e] Department of Economics, Finance, Regional and International Research, Opole University of Technology, ul. Luboszycka 7, 45-036 Opole, Poland

ARTICLE INFO

Article history:
Received 3 April 2021
Received in revised form
29 May 2021
Accepted 24 June 2021
Available online 29 June 2021

Keywords:
Waste utilization
Waste valorization
Hydrogen
Energy
Coal
Municipal waste

ABSTRACT

In the paper a novel approach to thermochemical utilization of low rank coal, flotation concentrates and municipal refuse derived fuels was presented. The economic attractiveness of low rank coals and flotation concentrates is limited and that is why they are commonly stored at excavation heaps causing additional costs and the risk of endogenous fires occurrence. One of the crucial parameters determining the attractiveness and usability of a fuel in the gasification process is its reactivity. In the study several low rank coals, flotation concentrates and municipal refuse derived fuels were tested in terms of their reactivity in the process of steam gasification. The reactivity of low rank coal and flotation concentrates at 50% of carbon conversion, R_{50}, varied between $1.46 \cdot 10^{-4}$ and $2.39 \cdot 10^{-4}$ s^{-1}, whereas the maximum reactivity, R_{max}, from $3.28 \cdot 10^{-4}$ to $4.62 \cdot 10^{-4}$ s^{-1}. Advanced mathematical models were developed to investigate the similarities and dissimilarities between the studied fuels as well as the relationships between the physical and chemical parameters and the reactivities of fuel chars in steam gasification. On this basis, a low rank coal was selected and blended with 20%$_{w/w}$ of municipal refuse derived fuel in co-gasification experiments. The aim of the research was to utilize the low rank coal characterized by the lowest reactivities (R_{50} and R_{max} of $1.46 \cdot 10^{-4}$ and $3.28 \cdot 10^{-4}$ s^{-1}, respectively) in steam co-gasification to hydrogen-rich gas with an alternative fuel in a fixed bed reactor at the temperature of 800 °C. The selected low rank coal was blended with 20%$_{w/w}$ of municipal refuse derived and the resulting fuel yielded the average concentration of hydrogen in the produced gas of 58.99%$_{vol}$.

1. Introduction

The main objective of the established EU 2020 Green Deal is that the European Union should become carbon neutral by 2050 [1]. It means that all fossil fuel energy sources must be replaced by the renewable ones. This goal seems to be a great challenge for all the European countries. Poland where almost 73.6% of electricity (in 2019) was generated from coal will have to transform its whole energy sector [2,3], which constitutes an extremely ambitious target. During last year, the decarbonatization process significantly speeded up in the EU. The new low-carbon technologies as well as zero-emission technologies must be implemented [4]. One of the very promising ways in terms of the decarbonization efforts is the application of a new, environmentally friendly energy carrier – hydrogen [5–8]. Unfortunately, 76% of globally produced hydrogen comes from fossil fuels (mainly through methane steam reforming) [9,10]. Currently, all the efforts are focused on the development and commercialization of the green hydrogen technologies based on photovoltaics (PV) [11] and wind power (onshore [12] and offshore [12,13]). Poland is one of the biggest producers of hydrogen. Unfortunately, this is the so-called grey hydrogen produced mainly through methane reforming [9,10]. Based on the Polish Hydrogen Strategy [14], this situation will change by the application of new technologies of water electrolysis using power produced from PV and offshore wind farms. Within the long term strategy, all hydrogen produced in Poland will come from the renewable

* Corresponding author.
E-mail address: smolin@gig.katowice.pl (A. Smoliński).

https://doi.org/10.1016/j.energy.2021.121348

sources. In the short and middle term, the hydrogen will be still produced from fossil fuels (methane and coal) [14].

Nowadays, hydrogen is produced in Poland only from coal and methane. Methane based hydrogen production generates CO_2 emission above 5.8 kg CO_2 eq/kg H_2 and above 10 kg CO_2 eq/kg H_2 [14,15] in the case coal is the source of primary energy. Within the Polish context, hydrogen bears the potential option of increasing the flexibility of conventional power plants through optimizing their cooperation with intermittent sources of energy. In future perspective, the assumed target is to replace the conventional energy sector with nuclear power plants as well as the PV and offshore wind farms. In a longer time perspective – by the year 2040, large expectations are associated with small scale high temperature nuclear reactors (HTR) [16–18] as well as small modular reactors (SMR) [19] for industrial applications as units generating high parameter process heat to enhance the decarbonization of the sector and to produce zero-emission hydrogen. However, in the coming years it is the co-gasification of coal, biomass and waste in order to generate a more environmentally friendly energy carrier that is considered to be the most promising option [20,21]. An urgent issue to be currently addressed is the utilization of low rank coal deposited at the extractive waste dumps coupled with large amounts of flotation concentrates generated during coal processing; the same applies to the steadily increasing volumes of municipal refuse [22,23]. In light of the gradual implementation of circular economy, the co-gasification of coal, biomass and waste in order to produce hydrogen rich gas seems to be an attractive pathway towards sustainability. It is not a coincidence that the gasification of solid fuels is mentioned as one of the prospective processes of energy sourcing which is in line with the rules of sustainable development [23].

In the literature there are numerous studies on thermal utilization of municipal waste in pyrolysis and gasification [24–26]. The studies on pyrolysis and gasification of the municipal refuse derived fuel fucus mainly on the effects of various operating parameters [24,25], gasification agents [28], temperature and pressure [27], metal oxides as catalysts and various reactor types [28] on the yield and composition of the product gas. The number of studies reported on thermal utilization of low rank coal and flotation concentrates is more limited [29]. At the same time, the efforts aiming at decreasing fossil fuel dependence generate a growing interest in co-utilization of coal and the renewables, among the others, in the process of co-gasification [30]. The same idea could be applied to co-gasification of low rank coals with waste to hydrogen-rich gas [31]. The study presented in the paper was focused on proving the feasibility of effective co-utilization of a municipal refuse derived fuel with low rank coal and flotation concentrates in co-gasification. The main aim of the study was to contribute to the development of a new method of thermal utilization of low rank coals, flotation concentrates and municipal refuse derived fuels to hydrogen-rich gas. Several low rank coals were tested in terms of the reactivity in gasification process and based on these results the coal for further co-gasification with municipal refuse derived fuel to hydrogen-rich gas was selected.

2. Materials and methods

2.1. Materials

The studied low rank coals (objects nos. 1, 2 and 5–14, denoted as CS) and flotation concentrates (objects nos. 3 and 4, denoted as FC) were provided by eight coal mines located in the Upper Silesia Coal Basin, Poland. The municipal waste was provided by one of the Upper Silesian municipalities (sample no. 15, denoted as MW). The physical and chemical parameters of the samples tested were determined by the accredited laboratory of the Central Mining Institute in accordance with the relevant standards: PN-G-04511:1980 (total moisture), PN-G-04560:1998 and PN-ISO 1171:2002 (ash), PN-G-04516:1998 and PN ISO-562:2000 (volatiles), PN-G-04513:1981 (heat of combustion, calorific value), PN-G-04571:1998 (carbon, hydrogen and nitrogen), and PN-G-04516:1998 (fixed carbon). The results are given in Table 1.

2.2. Experimental procedure

The experimental campaign was divided into two parts. In the first one the reactivity of the studied fuels and the municipal refuse derived fuel were tested in a fixed bed gasifier. Based on the reactivity, the optimal coal was used for further experimental works oriented on its co-gasification with municipal refuse derived fuel. The selected fuel blends with municipal refuse derived fuel were co-gasified under the atmospheric pressure in a laboratory scale installation with a fixed bed reactor. The experimental installation with a fixed bed reactor for solid fuels gasification is presented in Fig. 1. The fixed-bed reactor was designed in the shape of a cylinder of the external dimensions of 300 × 60 mm.

2.2.1. Fuel reactivity tests

The 3g dried fuel samples in analytical state with a grain size below 0.2 mm were put at the bottom of the reactor and heated under inert gas atmosphere (nitrogen) to the set temperature (800 °C) with a heating rate of 1.33 °C/s. When the set temperature was stabilized, the steam was injected to the reactor with the flow rate of 3.2 cm^3/min. The amount of the produced gas as well as its composition were monitored by a mass flowmeter and a gas chromatograph, respectively. The composition of the main gas components was measured using a two-channel gas chromatograph Agilent 3000A with a PLOT U column ($8 \cdot 10^{-3} \cdot 0.32 \times 10^{-3}$ m) equipped with a thermal conductivity detector (TCD) for the determination of carbon dioxide and hydrocarbons (up to 5 carbon atoms content in the molecule) and an analytical column MS5A PLOT ($10 \times 0.32 \cdot 10^{-3}$ m) with TCD for the determination of hydrogen, nitrogen, carbon monoxide and methane concentrations, respectively. Helium and argon were applied as carrier gases in the PLOT U and MS5A PLOT columns, respectively. The sample inlet and the injector temperature was 60 °C. The injection time was 50 ms for both columns (PLOT U and MS5A PLOT), whereas the columns temperature was 60 °C. The run time and the post run time was 150 s and 10 s, respectively, for both columns, whereas the backflush time was 12 s for column PLOT U. The reactivity of coal char for 50% of carbon conversion (R_{50}) as well as the maximal value of reactivity (R_{max}) were calculated as follows:

$$R_x = \frac{1}{m_0} \cdot \frac{dm}{dt_x} [s^{-1}] \quad (1)$$

where R_x describes the reactivity for X% of carbon conversion, m_0 describes the carbon content in the fuel sample, m describes the carbon content in the gas produced in the gasification process and t_x denotes time needed to achieve X% of carbon conversion ($X = m/m_0 \cdot 100\%$). Moreover, the times needed to reach R_{50} and R_{max} were also determined.

2.2.2. Co-gasification tests

The 10 g coal sample blend with municipal refuse derived fuel in the analytical state was put at the bottom of the reactor between the quartz wool. In the first stage of the experiment, the reactor was heated in nitrogen atmosphere to the set temperature (800 °C). The heating rate was set as 1.33 °C/s. When the temperature had stabilized, steam was injected in the inert gas atmosphere into the

Table 1
The physical and chemical properties of tested fuels.

No	Sample	Moisture%	Ash %	Volatiles %	Heat of combustion kJ/kg	Calorific value kJ/kg	S %	C %	H %	N %	O %	Ash fusion temperatures, °C							
												sintering		softening		melting		flow	
												o	r	o	r	o	r	o	r
1	CS1	1.32	2.66	32.18	33,697	32,506	0.29	82.19	5.31	1.52	6.89	1040	960	1340	1280	1350	1320	1400	1360
2	CS2	1.39	2.81	30.23	33,604	32,531	0.31	83.62	4.76	1.35	5.94	1020	950	1250	1180	1300	1200	1360	1230
3	FC1	1.74	4.47	27.38	32,745	31,663	0.42	80.16	4.76	1.35	7.28	960	920	1220	1160	1280	1230	1320	1300
4	FC2	2.25	15.49	26.50	27,705	26,744	0.51	69.71	4.15	1.10	6.92	970	890	1260	1220	1490	1430	>1500	1480
5	CS3	9.70	6.66	31.69	26,264	25,115	1.59	67.61	4.18	0.99	9.70	930	880	1300	1130	1360	1160	1400	1180
6	CS4	9.40	10.82	29.33	24,938	23,820	1.83	64.27	4.07	0.95	9.06	940	910	1270	1170	1300	1220	1330	1280
7	CS5	7.77	9.52	30.91	26,076	24,984	1.67	67.32	4.13	0.99	8.72	970	900	1330	1280	1460	1420	1500	1450
8	CS6	7.50	7.85	31.67	27,170	26,066	0.90	68.14	4.22	1.02	11.09	950	1140	1350	1330	1360	1360	1380	1360
9	CS7	5.79	5.48	35.10	28,914	27,744	0.77	71.52	4.71	1.08	11.17	950	1140	1370	1350	1380	1370	1400	1380
10	CS8	1.65	4.64	27.73	33,166	32,037	0.51	80.20	4.99	1.43	6.73	1050	1000	1270	1230	1320	1310	1360	1340
11	CS9	1.60	1.86	33.54	33,652	32,476	0.31	82.53	5.21	1.50	7.17	1020	960	1340	1300	1380	1360	1420	1370
12	CS10	1.85	2.05	28.42	33,484	32,369	0.30	82.44	4.90	1.48	7.18	1100	1050	1350	1330	1370	1360	1420	1370
13	CS11	1.53	18.24	32.15	27,907	26,881	0.84	69.97	4.53	1.27	3.92	990	940	1380	1350	1460	1440	1480	1460
14	CS12	1.17	1.66	31.31	34,923	33,770	0.27	85.59	5.15	1.48	4.74	1070	980	1290	1240	1350	1300	1430	1340
15	MW	1.99	15.69	75.07	25,730	24,267	0.26	56.18	6.88	0.88	N/A	N/A	N/A	N/A	N/A	N/A	N/A	N/A	N/A

o – oxidizing atmosphere, r – reducing atmosphere.

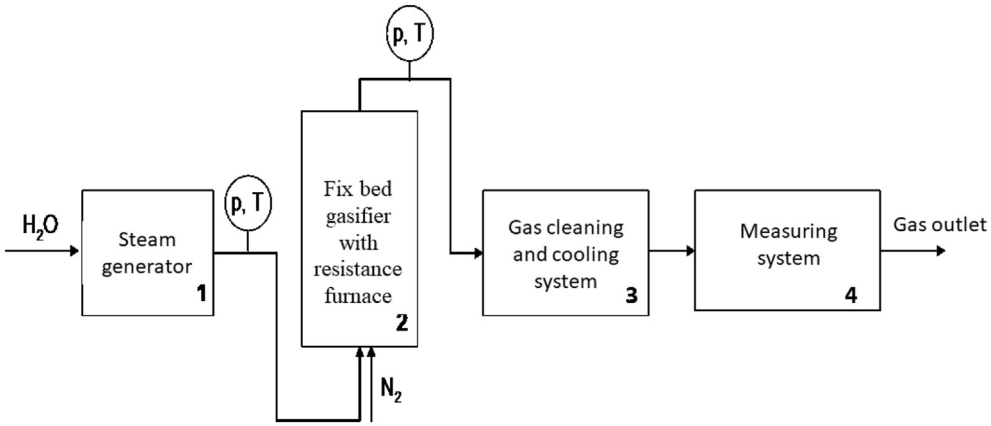

Fig. 1. Lab-scale installation for solid fuels gasification with the fixed-bed reactor (1- steam generator, 2- fix bed gasifier with resistance furnace; 3- gas cleaning and cooling system; 4 - measuring system – gas flowmeter and gas chromatograph, respectively).

reaction chamber with a flow rate of 3.2 ml/min. The produced gas was cooled and dried in a water trap. All condensed liquid products were collected at the bottom of the water trap, whereas the clean, cold gas was analyzed online with a gas chromatograph Agilent 3000A. Moreover, the amount of the produced gas was also determined by means of a mass flowmeter. The experiment was repeated three times.

3. Results and discussion

The first stage of the experiment was oriented on the selection of the best low rank coal for further gasification tests. The gasification seems to be an attractive alternative for the combustion process which is considered as problematic mainly due to the economic as well as environmental concerns. Naturally, low-grade coal is cheaper but its combustion leads to a significant increase in the emission of greenhouse gases. In addition, burning low rank coal is the main cause of smog in Poland during the winter season. Nowadays, Polish law regulations do not allow using low-quality coals in household boilers so their conversion into valuable products seems to be a huge challenge for coal producing companies. One of the viable options seems to be their gasification to achieve a marketable product such as hydrogen, a clean and environmentally friendly energy carrier. The selection of the optimal coal from the whole group of the tested low rank coals is a crucial issue. For that purpose, a systematic study of the reactivity of the studied low rank coal samples from different Polish coal mines located in the Upper Silesia Coal Basin was conducted. The selected low rank coal will be further used for studies oriented on the utilization of municipal refuse derived fuel in the co-gasification process oriented on hydrogen production. The values of the char reactivity, obtained for low rank coal and flotation concentrate in the gasification process at the temperature of 800 °C are presented in Table 2.

The reactivity of 50% of carbon conversion, R_{50}, varies between $1.46 \cdot 10^{-4}$ and $2.39 \cdot 10^{-4}$ s^{-1}, whereas the maximum reactivity, R_{max}, ranges from $3.28 \cdot 10^{-4}$ to $4.62 \cdot 10^{-4}$ 1/s. The carbon conversion rate in the 1-h coal char gasification trial varied from 69.23 to 76.56% CS5 and CS12, respectively. Coal sample CS1 was characterized by the lowest reactivity R_{50} and R_{max} among all the studied samples. The values of R_{50} and R_{max} measured for the studied flotation concentrates FC1 and FC2 (samples nos. 3 and 4) were similar to the values calculated for the remaining low rank coals. The main objective of this part of the research was to select the coal sample for further co-gasification tests with refuse derived fuel. The reactivity was an important parameter but not the only one that determined the optimal selection of the proper fuel for the gasification process. All the tested fuels were characterized by the physico-chemical parameters essential from the thermo-chemical

Table 2
Low rank coal and flotation concentrate chars reactivity for 50% of carbon conversion, R_{50}, and the maximum reactivity, R_{max}, with the time needed to achieve R_{50}, t_{50}, and the R_{max}.

No.	Studied char sample	R_{50} [1/s]	R_{max} [1/s]	t_{50} [s]	t_{max} [s]
1	CS1	$1.46 \cdot 10^{-4}$	$3.28 \cdot 10^{-4}$	2292	534
2	CS2	$1.59 \cdot 10^{-4}$	$3.36 \cdot 10^{-4}$	2370	546
3	FC1	$1.89 \cdot 10^{-4}$	$3.29 \cdot 10^{-4}$	2112	540
4	FC2	$1.92 \cdot 10^{-4}$	$3.78 \cdot 10^{-4}$	1926	426
5	CS3	$1.72 \cdot 10^{-4}$	$3.92 \cdot 10^{-4}$	1830	396
6	CS4	$1.99 \cdot 10^{-4}$	$4.01 \cdot 10^{-4}$	1692	372
7	CS5	$2.04 \cdot 10^{-4}$	$4.11 \cdot 10^{-4}$	1794	360
8	CS6	$1.80 \cdot 10^{-4}$	$3.82 \cdot 10^{-4}$	1926	372
9	CS7	$1.74 \cdot 10^{-4}$	$3.83 \cdot 10^{-4}$	2022	505
10	CS8	$1.63 \cdot 10^{-4}$	$3.40 \cdot 10^{-4}$	2202	516
11	CS9	$1.47 \cdot 10^{-4}$	$3.43 \cdot 10^{-4}$	2322	474
12	CS10	$1.75 \cdot 10^{-4}$	$3.51 \cdot 10^{-4}$	2167	492
13	CS11	$2.32 \cdot 10^{-4}$	$4.49 \cdot 10^{-4}$	1656	354
14	CS12	$2.39 \cdot 10^{-4}$	$4.62 \cdot 10^{-4}$	2196	534

processing point of view (see Table 1).

In order to perform a complex analysis of the studied data, the method of hierarchical clustering analysis (HCA) combined with a colour map of the data was applied [32–34]. Hierarchical clustering techniques complemented with visual display of data sets allow direct interpretation of the clustering results in terms of original variables. The HCA was employed to select the low-quality coal for the co-gasification tests with municipal refuse derived fuel. The hierarchical clustering method is composed of several iterative stages. In the first stage, the algorithm calculates the similarity between the studied samples (characterized by the studied parameters) based on a similarity metric. In our study, the Euclidean distance was used as a similarity measure. Based on this calculation, the dendrogram was built. The crucial thing is that the most similar samples were grouped and they cannot be considered separately. These samples are treated as one and the similarity is determined between all the remaining samples and the newly created group. In order to perform the hierarchical clustering analysis, the data were organized into matrix $\mathbf{X}(14 \times 22)$, where the rows represent the studied samples (listed in Tables 1 and 2) and the columns represent the studied physico-chemical parameters which characterized the studied coal samples and the calculated values of R_{50} and R_{max} as well as the measured time needed to reach R_{50} and R_{max}, respectively (see Table 3).

As mentioned above, the selection of the optimal fuel for further processing in the co-gasification with municipal refuse derived fuel must be preceded by an in-depth analysis of the studied fuels, both in terms of their reactivities and their physical and chemical characterization. The HCA was applied to tracing the relationships between chars reactivity and the remaining parameters. For that purpose, the Ward's linkage algorithm based on the Euclidean distance was used. The dendrograms of the studied samples (objects) in the space of 22 measured parameters (listed in Table 2) and the parameters in the object space are presented in Fig. 2.

At the dendrogram presented in Fig. 2a, it is possible to distinguish three clusters of the studied samples. Cluster A is composed of fuel samples CS1, CS2, FC1, XC8, CS8, CS9, CS10 and CS12 (objects nos. 1–3, 10–12 and 14), cluster B collects fuel samples FC2, CS5 and CS11 (objects nos. 4, 7 and 13), whereas cluster C is composed of fuel samples CS3, CS4, CS6 and CS7 (objects nos. 5, 6, 8 and 9). Moreover, two of the mentioned clusters have an additional substructure. Namely, within cluster A, the following two subclusters can de observed:

- sub-cluster A1 which is composed of fuel samples CS1, CS9, CS10 and CS12 (objects nos. 1, 11, 12 and 14), and
- sub-cluster A2 which collects fuel samples CS2, FC1 and CS8 (objects nos. 2, 3 and 10).

Table 3
Parameters characterizing studied low-quality coal and flotation concentrate with the R_{50} and R_{max} calculation analyzed with HCA.

No.	Parameter	Unit
1	Total moisture content	%
2	Ash content	%
3	Volatiles content	%
4	Heat of combustion	$kJ \cdot kg^{-1}$
5	Calorific value	$kJ \cdot kg^{-1}$
6	Total sulfur	%
7	Carbon	%
8	Hydrogen	%
9	Nitrogen	%
10	Oxygen	%
11	Sintering point (oxy)	^0C
12	Sintering point (red)	^0C
13	Softening point (oxy)	^0C
14	Softening point (red)	^0C
15	Melting point (oxy)	^0C
16	Melting point (red)	^0C
17	Flow temp. (oxy)	^0C
18	Flow temp. (red)	^0C
19	Reactivity for 50% of carbon conversion R_{50}	s^{-1}
20	Time to reach R_{50}, t_{50}	s
21	Maximum reactivity R_{max}	s^{-1}
22	Time to reach R_{max}, t_{max}	s

Within cluster C, it is possible to observe sub-cluster C1 (composed of fuel samples CS3 and CS4 – objects nos. 5 and 6) and sub-cluster C2 (comprising fuel samples CS6 and CS7 – objects nos. 8 and 9). In a similar way, the dendrogram, constructed for studied parameters in the space of 14 objects (see Fig. 2b), allows grouping the studied parameters into 4 main classes:

- class A collecting parameters nos. 4, 5, 7–9, 11, 20 and 22 (describing Heat of combustion, Calorific value, Carbon, Hydrogen and Nitrogen content, Sintering point (oxy), Time to reach R_{50}, t_{50} and Time to reach R_{max}, t_{max});
- class B grouping parameters nos. 1, 6 and 10 (describing Total moisture content, Total sulfur and oxygen content);
- class C containing parameters nos. 3, 12, 13 and 14 (representing Volatiles content, Sintering point (red) and Softening point (oxy) and (red);
- class D constituting parameters nos. 2, 15–19 (describing Ash content, Melting point (oxy) and (red), Flow temp. (oxy) and (red) and Reactivity for 50% of carbon conversion, R_{50}.

The dendrograms allow to investigate the data structure such as the clustering or sub-clustering of the studied fuels samples or to investigate the grouping of the analyzed parameters. Unfortunately, HCA does not allow explaining the observed objects' patterns in terms of the studied parameters. This disadvantage could be overcome by adding the color map of the studied data (see Fig. 2c) sorted according to the order of objects and parameters shown on the dendrograms presented in Fig. 2a and b.

Based on the simultaneous interpretation of the dendrograms presented in Fig. 2a and the color map of the studied data, a conclusion may be drawn that all fuel samples collected in cluster A are characterized by higher heat of combustion, calorific value, carbon, hydrogen and nitrogen content in the fuel sample, higher sintering point temperature measured in the oxidation atmosphere, longer time to reach R_{50} (t_{50}) and R_{max} (t_{max}), respectively (parameters nos. 4, 5, 7–9, 11, 20 and 22) as well as lower values of such parameters as total moisture, ash and total sulfur content in

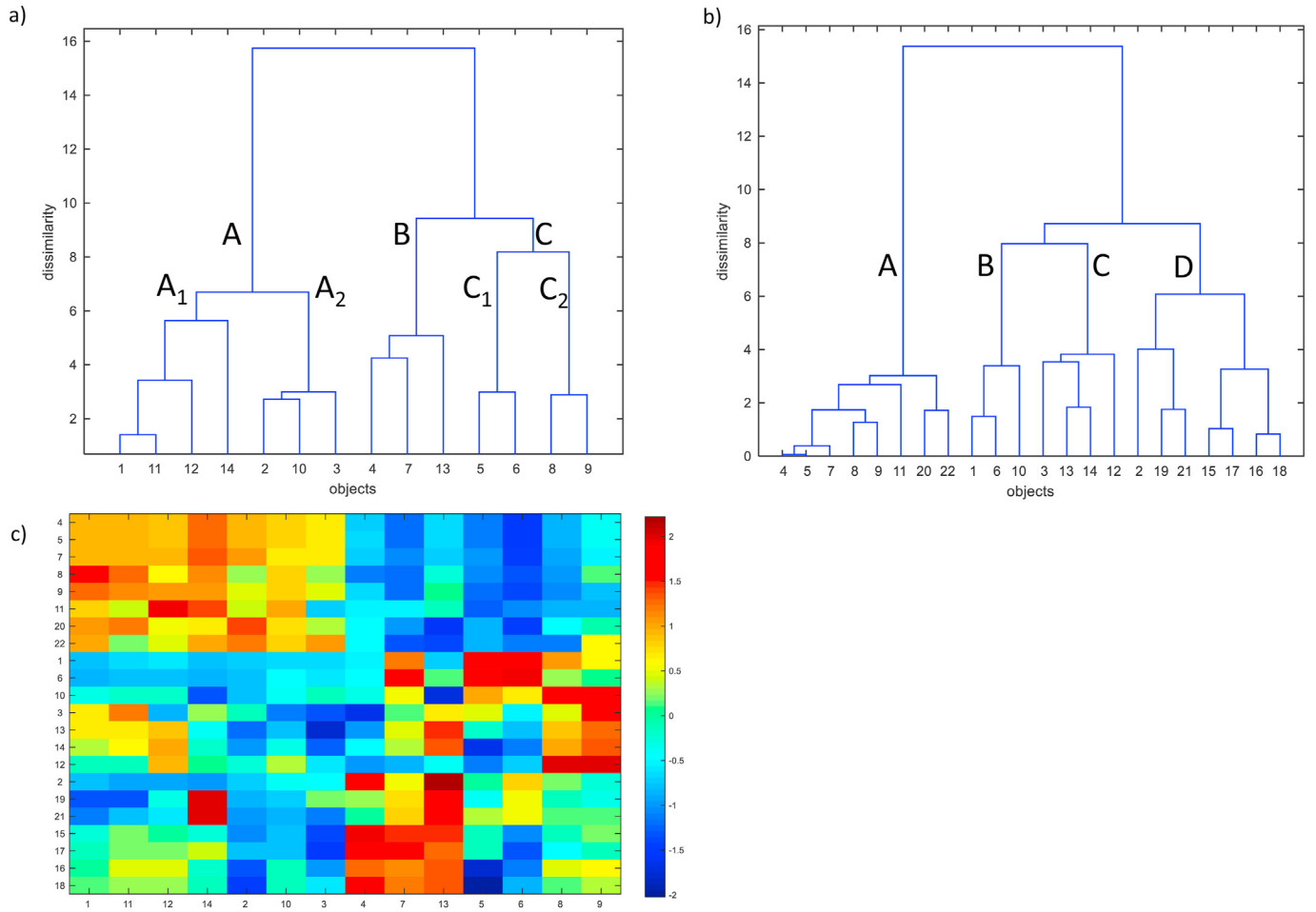

Fig. 2. Dendrograms of (a) studied samples (objects) in the space of 22 measured parameters and (b) parameters in the space of 14 objects with (c) the color map of the studied data sorted according to the Ward linkage method. (For interpretation of the references to color in this figure legend, the reader is referred to the Web version of this article.)

the sample (parameters nos. 1, 2 and 6) in comparison with all the remaining fuel samples. Coal samples CS1, CS9, CS10, and CS12 (objects nos. 1, 11, 12 and 14) collected in sub-cluster A1 are additionally unique due to the relatively high volatile content and the temperature of sintering point measured in the reduction atmosphere and softening, melting and flow temperatures, both in the oxidation and reduction atmosphere, respectively (parameters nos. 3, 12–18). Furthermore, coal sample CS10 (object no. 12) is characterized by the highest sintering point temperature in the oxidation atmosphere (parameter no. 11) and the lowest reactivity for 50% of carbon conversion, R_{50} (parameter no. 19) among all the studied fuel samples. Likewise coal sample CS12 (object no. 14), it is characterized by the highest heat of combustion, calorific value, carbon content and the highest value of reactivity for 50% of carbon conversion, R_{50}, and maximum reactivity, R_{max}, respectively (parameters nos. 4, 5, 7, 19 and 21), whereas coal sample CS1 (object no. 1) is characterized by the highest hydrogen and nitrogen content in the sample (parameters nos. 8 and 9). Sub-cluster A2 has been characterized by a relatively low melting point and flow temperature in the oxidation atmosphere, respectively and the low value of maximum reactivity, R_{max} (parameters nos. 15, 17 and 21) among all the studied fuel samples. Again, the uniqueness of coal sample CS2 and flotation concentrate FC1 (objects nos. 2 and 3) could be also observed. Namely, flotation concentrate FC1 (object no. 3) is differed from all the remaining samples mainly due to the lowest softening, melting points and flow temperature in the oxidation atmosphere, respectively (parameters nos. 13, 15 and 17), whereas coal sample CS2 is unique due to the longest time needed to reach R_{50} (t_{50}) and R_{max} (t_{max}), respectively (parameters nos. 20 and 22).

All the fuel samples collected in cluster B could be described by a relatively high melting point and flow temperatures, both in the oxidation and reduction atmosphere (parameters nos. 15–18) among all the studied samples. Similarly to cluster A, the uniqueness of several fuel samples could be also observed. Namely, flotation concentrate FC2 (object no. 4) is unique due to the highest and the lowest values of melting point and softening point in the oxidation atmosphere (parameters nos. 15 and 13), respectively. Moreover, coal sample CS11 (object no. 13) is additionally characterized by the highest ash content and the highest softening point in the oxidation and reduction atmosphere, respectively (parameters nos. 2, 13 and 14) among all the studied fuel samples.

Fuels samples collected in cluster C are characterized by the relatively lower heat of combustion, calorific value, carbon, hydrogen and nitrogen content in the fuel sample and higher sintering point temperature measured in the oxidation atmosphere, respectively (parameters nos. 4, 5, 7–9, and 11) in comparison with all the remaining fuel samples. Sub-cluster C1 which groups two coal samples – CS3 and CS4 (objects nos. 5 and 6) is unique due to the relatively highest total moisture and total sulfur content in the studied samples (parameters nos. 1 and 6) and the lower melting point and flow temperature in the reduction atmosphere

(parameters nos. 16 and 18) in comparison with all the remaining studied fuels. The uniqueness of coal sample CS3 (object no. 5) is caused due to the lowest softening point, melting point and flow temperature in the reduction atmosphere, respectively (parameters nos. 14, 16 and 18) and the highest total sulfur content (parameter no. 6) among all the studied samples. Sub-cluster C2 is characterized by the highest value of sintering point in the reduction atmosphere (parameter no. 12). Moreover, coal sample CS7 (object no. 9) is exceptional due to the highest volatiles content (parameter no. 3) among all the studied samples.

Based on the in-depth analysis of the reactivities for 50% of carbon conversion as well as the maximum reactivity measured for the obtained chars combined with the analysis of the physical and chemical parameters important from the gasification point of view, the fuel sample with the lowest value of reactivity was selected for further co-gasification step.

The lowest reactivities R_{50} and R_{max} equal to $1.46 \cdot 10^{-4}$ and $3.28 \cdot 10^{-4}$ 1/s, respectively were observed for low rank coal sample CS1. Coals with the lowest reactivity are hardly commercially viable. One of the promising options for their utilization is their use in the co-gasification process with municipal refuse derived fuel combined with the production of hydrogen, a clean and environmentally friendly energy carrier. One-process utilization of low rank coal and municipal refuse derived fuel, including biodegradable materials as well as plastics, seems to be a mutually beneficial choice from the environmental and economic point of view.

In our study, the co-gasified fuel contains $20\%_{w/w}$ of municipal refuse derived fuel which seems to be a very attractive option of their utilization. Moreover, in the steam co-gasification process of low-rank coal blended with municipal refuse derived fuel, hydrogen rich gas is produced. Hydrogen which could be obtained in the course of the process bears the potential to be applied in the energy or transportation sectors. Fig. 3 presents the average total volumes of the main components of the gas produced in the co-gasification of coal blends with municipal refuse derived fuel at the temperature of 800 °C.

The studied co-gasification stage was repeated three times. In the experimental trial, we produced in total 5791 cm^3 of gas composed in $59\%_{vol.}$ of hydrogen from 10g of the tested fuel (containing $20\%_{w/w}$ of municipal refuse derived fuel). It is possible to conclude that the higher temperature enforces the endothermic reactions for products formation. Namely, the increase of the steam/biomass ratio lead to increase the H_2 and CO_2 formations as well as decreases CO formation [35]. The low concentration of CH_4 in the produced gas is caused by steam and dry methane reforming. Based on the average composition of the produced gas and the average total amount produced in the co-gasification tests, the calorific value of the produced gas was calculated as follows:

$$Q_g = \sum_i c_i \cdot W_i \ [kJ \cdot kg^{-1}] \quad (2)$$

where c_i describes the concentration of the particular component in the produced gas in $\%_{mass}$, while W_i describes the heat of combustion in $kJ \cdot kg^{-1}$. The average calculated value of Q_g of the produced gas was 13,753 kJ/kg. Additionally, the ratio of the energy output in the produced gas to the energy input in coal equaled 0.45.

4. Conclusions

In the paper an alternative solution for the use of low rank coal with simultaneous utilization of municipal refuse derived fuel was proposed. The co-gasification of the worst low rank coal (among all the studied ones) blends with $20\%_{w/w}$ of municipal refuse derived fuel allows to produce hydrogen rich gas. The concentration of hydrogen in the produced gas was $59\%_{vol}$. The low rank coal of the worst quality was selected from 14 tested coal samples (low rank coals and flotoconcentrate) based on the application of HCA. In the analysis, not only the reactivity but also all the physico-chemical parameters important from the gasification point of view, were analyzed simultaneously. The proposed idea of utilizing thermochemically low rank coal and municipal refuse derived fuel seems to be a promising option in addressing the issues of municipal waste management and the commercial utilization of poor quality fuels like low rank coals and flotoconcentrate. The simultaneous production of a marketable product – hydrogen rich gas may be considered from the economic and especially environmental point of view as an added value.

Credit author statement

Adam Smoliński: Conceptualization, Methodology, Investigation, Formal analysis, Data curation, Writing – original draft, Writing – review & editing, Supervision, Natalia Howaniec: Conceptualization, Methodology, Investigation, Formal analysis, Rafał Gąsior: Formal analysis, Visualization, Investigation. Jarosław Polański: Conceptualization, Formal analysis, Małgorzata Magdziarczyk: Conceptualization, Formal analysis

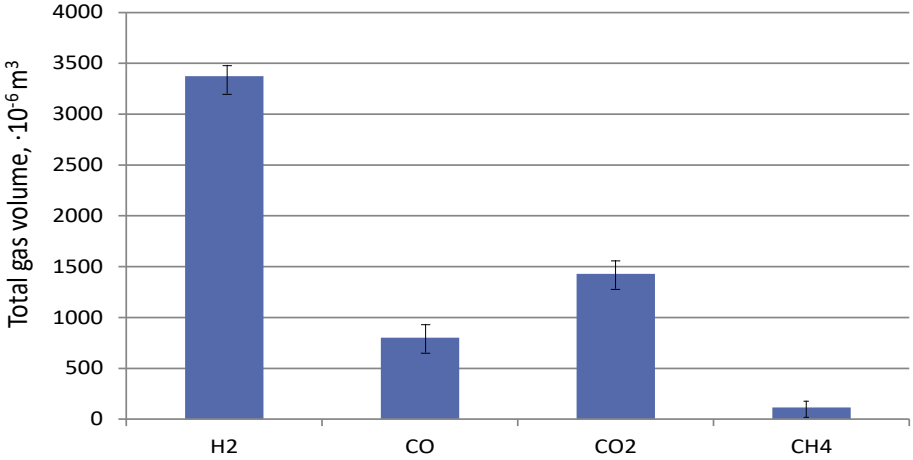

Fig. 3. Total gas volume of the main gas component in the steam co-gasification process at temperature 800 °C.

Declaration of competing interest

The authors declare that they have no known competing financial interests or personal relationships that could have appeared to influence the work reported in this paper.

References

[1] Papadis E, Tsatsaronis G. Challenges in the decarbonization of the energy sector. Energy 2020;205:118025. https://doi.org/10.1016/j.energy.2020.118025.

[2] Żuk P, Żuk P, Pluciński P. Coal basin in Upper Silesia and energy transition in Poland in the context of pandemic: the socio-political diversity of preferences in energy and environmental policy. Resour Pol 2021;71:101987. https://doi.org/10.1016/j.resourpol.2021.101987.

[3] Brauers H, Oei PY. The political economy of coal in Poland: drivers and barriers for a shift away from fossil fuels. Energy Pol 2020;144:111621. https://doi.org/10.1016/j.enpol.2020.111621.

[4] Pye S, Li PH, Keppo I, O'Gallachoir B. Technology interdependency in the United Kingdom's low carbon energy transition. Energy Strat Rev 2019;24:314–30. https://doi.org/10.1016/j.esr.2019.04.002.

[5] Chuayboon S, Abanades S. An overview of solar decarbonization processes, reacting oxide materials, and thermochemical reactors for hydrogen and syngas production. Int J Hydrogen Energy 2020;45:25783–810. https://doi.org/10.1016/j.ijhydene.2020.04.098.

[6] Smoliński A, Howaniec N, Bąk A. Utilization of energy crops and sewage sludge in the process of co-gasification for sustainable hydrogen production. Energies 2018;11:809. https://doi:10.3390/en11040809.

[7] Howaniec N, Smoliński A. Effect of fuel blend composition on the efficiency of hydrogen-rich gas production in co-gasification of coal and biomass. Fuel 2014;128:442–50. https://doi.org/10.1016/j.fuel.2014.03.036.

[8] Gautier M, Rohani V, Fulcheri L. Direct decarbonization of methane by thermal plasma for the production of hydrogen and high value-added carbon black. Int J Hydrogen Energy 2017;42:28140–56. https://doi.org/10.1016/j.ijhydene.2017.09.021.

[9] Navas-Anguita Z, García-Gusano D, Dufour J, Iribarren D. Revisiting the role of steam methane reforming with CO2 capture and storage for long-term hydrogen production. Sci Total Environ 2021;771:145432. https://doi.org/10.1016/j.scitotenv.2021.145432.

[10] Howaniec N, Smoliński A. Steam co-gasification of coal and biomass - synergy in reactivity of fuel blends chars. Int J Hydrogen Energy 2013;38:16152–60. https://doi.org/10.1016/j.ijhydene.2013.10.019.

[11] Peláez-Peláez S, Colmenar-Santo A, Pérez-Molina C, Rosales AE, Asensio AE. Techno-economic analysis of a heat and power combination system based on hybrid photovoltaic-fuel cell systems using hydrogen as an energy vector. Energy 2021;224:120110. https://doi.org/10.1016/j.energy.2021.120110.

[12] Schnuelle C, Wassermann T, Fuhrlaender D, Zondervan E. Dynamic hydrogen production from PV & wind direct electricity supply – modeling and techno-economic assessment. Int J Hydrogen Energy 2020;45:29938–52.

[13] Dinh VB, Leahy P, McKeogh E, Murphy J, Cummins V. Development of a viability assessment model for hydrogen production from dedicated offshore wind farms. Int J Hydrogen Energy 2020. https://doi.org/10.1016/j.ijhydene.2020.04.232.

[14] Polish hydrogen strategy to 2030 with the 2040 perspective. https://www.teraz-srodowisko.pl/media/pdf/aktualnosci/9801-Projekt-Polskiej-Strategii-Wodorowej-do-roku-2030-z-perspektywa-do-2040-r.pdf.

[15] Ahmed U, Zahid U, Lee Y. Process simulation and integration of IGCC systems for H2/syngas/electricity generation with control on CO2 emissions. Int J Hydrogen Energy 2019;44:7137–48. https://doi.org/10.1016/j.ijhydene.2019.01.276.

[16] Norouzi N, Talebi S, Fani M, Khajehpour H. Exergy and exergoeconomic analysis of hydrogen and power cogeneration using an HTR plant. Nucl Eng Technol 2021. https://doi.org/10.1016/j.net.2021.02.027.

[17] Krawczyk P, Howaniec N, Smoliński A. Economic efficiency analysis of substitute natural gas (SNG) production in steam gasification of coal with the utilization of HTR excess heat. Energy 2016;114:1207–13. https://doi.org/10.1016/j.energy.2016.08.088.

[18] Howaniec N, Smoliński A, Cempa-Balewicz M. Experimental study of nuclear high temperature reactor excess heat use in the coal and energy crops co-gasification process to hydrogen-rich gas. Energy 2015;84:455–61. https://doi.org/10.1016/j.energy.2015.03.011.

[19] Yan Y, Thanganadar D, Clough PT, Mukherjee S, Patchigolla K, Manovic V, Anthony EJ. Process simulations of blue hydrogen production by upgraded sorption enhanced steam methane reforming (SE-SMR) processes. Energy Convers Manag 2020;222:113144. https://doi.org/10.1016/j.enconman.2020.113144.

[20] Cabuk B, Duman G, Yanik J, Olgun H. Effect of fuel blend composition on hydrogen yield in co-gasification of coal and non-woody biomass. Int J Hydrogen Energy 2020;45:3435–43. https://doi.org/10.1016/j.ijhydene.2019.02.130.

[21] Smoliński A, Howaniec N. Co-gasification of coal/sewage sludge blends to hydrogen-rich gas with the application of the simulated high temperature reactor excess heat. Int J Hydrogen Energy 2016;41:8154–8. https://doi.org/10.1016/j.ijhydene.2015.10.145.

[22] Park SW, Seo YC, Lee SY, Yang WS, Ohd JH, Gue JH. Development of 8 ton/day gasification process to generate electricity using a gas engine for solid refuse fuel. Waste Manag 2020;113:186–96. https://doi.org/10.1016/j.wasman.2020.06.004.

[23] Pio DT, Tarelho LAC, Tavares AMA, Matos MAA, Silva V. Co-gasification of refused derived fuel and biomass in a pilot-scale bubbling fluidized bed reactor. Energy Convers Manag 2020;206:112476. https://doi.org/10.1016/j.enconman.2020.112476.

[24] Nobre C, Vilarinho C, Alves O, Mendes B, Gonçalves M. Upgrading of refuse derived fuel through torrefaction and carbonization: evaluation of RDF char fuel properties. Energy 2019;181:66–76.

[25] Khosasaeng T, Suntivarakorn R. Effect of equivalence ratio on an efficiency of single throat downdraft gasifier using RDF from municipal solid waste. Energy Procedia 2017;138:784–8.

[26] Rocca S, van Zomeren A, Costa G, Dijkstr JJ, Comans RNJ, Lombardia F. Characterisation of major component leaching and buffering capacity of RDF incineration and gasification bottom ash in relation to reuse or disposal scenarios. Waste Manag 2012;32:759–68.

[27] Barba D, Capocelli M, Cornacchi G, Materac DA. Theoretical and experimental procedure for scaling-up RDF gasifiers: the Gibbs Gradient Method. Fuel 2016;179:60–70.

[28] Assim PG, Rose M, Jean R, Lavoie M. Role of fixed carbon and metal oxides in char during the catalytic conversion of tar from RDF gasification. Fuel 2018;218:406–16.

[29] Łabaj J, Blacha L, Smalcer A, Wieczorek J, Fröhlichová M, Vadasz P, Findorak R, Niesler M. Utilization of waste coal flotation concentrate for copper matte smelting, Engineering Science and Technology. Int J 2021;24:996–1004.

[30] Cormos CC. Hydrogen and power co-generation based on coal and biomass/solid wastes co-gasification with carbon capture and storage. Int J Hydrogen Energy 2012;37:5637–48. https://doi.org/10.1016/j.ijhydene.2011.12.132.

[31] Djaković-Sekulić T, Smolinski A, Perisić-Janjić N, Janicka M. Chemometric characterization of (chromatographic) lipophilicity parameters of newly synthesized s-triazine derivatives. J Chemometr 2008;22:195–202. https://doi.org/10.1002/cem.1111.

[32] Kaufman L, Rousseeuw PJ. Finding groups in data: an introduction to cluster analysis. John Wiley & Sons; 2009.

[33] Howaniec N, Smolinski A. Biowaste utilization in the process of co-gasification with bituminous coal and lignite. Energy 2017;118:18–23. https://doi.org/10.1016/j.energy.2016.12.021.

[34] Romesburg C. Cluster analysis for researchers. Lulu Press; 2004.

[35] Wang S, Luo K, Hu C, Sun L, Fan J. Impact of operating parameters on biomass gasification in a fluidized bed reactor: an Eulerian-Lagrangian approach. Powder Technol 2018;333:304–16. https://doi.org/10.1016/j.powtec.2018.04.027.